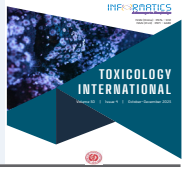
Toxicology International, *30(4) : 659-674; 2023. DOI: 10.18311/ti/2023/v30i4/35228*

Online ISSN : 0976-5131; Print ISSN : 0971-6580

Toxicology International

Contents available at: www.informaticsjournals.com/index.php/toxi



Assessment of Anti-Carcinogenic Potential of Neem (*Azadirachta indica*) Leaf Extract Loaded Calcium Phosphate Nanoparticles against Experimentally Induced Mammary Carcinogenesis in Rats

S. G. Chavhan*, C. Balachandran, A. P. Nambi, G. Dhinakar Raj and S. Vairamuthu

Department of Veterinary Pathology, Madras Veterinary College, Tamil Nadu Veterinary and Animal Sciences University, Chennai - 600 007, Tamil Nadu, India; drsam24183@gmail.com

Abstract

Considering the need for alternative medicine in alleviation of tumors and use of nanotechnology in furthering the action of herbal/natural products, the present study was designed to evaluate the anti-carcinogenic potential of Neem leaf Extract (NE) loaded calcium phosphate nanoparticles (NE-CaNP) on 7, 12-Dimethylbenzanthracene (DMBA) induced mammary tumors in female Sprague-Dawley rats. Ultrastructurally, the NE-CaNP were smooth, spherical with a tendency to agglomerate and evenly distributed. The NE-CaNP had a mean diameter of 231.4 ± 89.2 nm and zeta potential of -31.3mV. The mean coupling efficiency of CaNP was 90-91 %. The experimental trial consisted of control, NE-CaNP control, DMBA, DMBA+NE and DMBA+NE-CaNP groups. The mean latency periods for occurrence of mammary tumor were significantly ($P \leq 0.05$) increased in the DMBA+NE and DMBA+NE-CaNP groups compared to the DMBA group. The mean latency period in the DMBA+NE-CaNP group was significantly ($P \leq 0.05$) higher than the DMBA+NE group. The mean tumor frequency, volume and weight were significantly ($P \leq 0.05$) decreased in the DMBA+NE-CaNP group. Histopathologically, the number of benign lesions was found highest (47.54%) in DMBA+NE-CaNP group rats. The relative percent reduction in malignancy as compared to the DMBA group was 42.86% and 54.29% in the DMBA+NE and DMBA+NE-CaNP groups respectively. In conclusion, the neem leaf extract loaded calcium phosphate nanoparticles were found to have better anti-carcinogenic potential by significantly reducing the incidence, frequency, weight, volume, malignancy and increased the tumor latency period of DMBA induced mammary tumors in female Sprague-Dawley rats as compared to rats treated with neem extract alone. Findings of the present study suggested that the neem leaf extract loaded calcium phosphate nanoparticles (NE-CaNP) has immense anticancer potential in terms of reduction in tumor burden and malignancy.

Keywords: Calcium Phosphate Nanoparticles, DMBA, Mammary Tumor, Neem Leaf Extract, Rats

*Author for correspondence

Article Received on: 29.09.2023 Revised on: 09.11.2023 Accepted on: 09.11.2023

1. Introduction

Mammary tumors are the second most common tumor in dogs and has equal bearing in human breast cancer. Cancer is a highly complex disease to understand because it entails multiple cellular physiological systems. The most common cancer treatments are restricted to chemotherapy, radiation and surgery. Moreover, the early recognition and treatment of cancer remains a technological bottleneck. There is an urgent need to develop new and innovative technologies that could help to delineate tumor margins, identify residual tumor cells and micro metastases and determine whether a tumor has been completely removed or not[1].

Herbal plants and plants derived medicines have been used as the source of potential anti-cancerous agents in traditional cultures all over the world and are also becoming popular in modern society. The usage of natural products against tumors will avoid chemical toxicity and serves as an alternative medicine available for cancer therapy[2]. Neem *(Azadirachta indica)* is one such medicinal plant, the extract of which has been used for thousands of years for most acute and chronic diseases in India and Africa. The major biologically active constituents of neem leaves are limonoids, triterpenoids, non-terpenoids, phenolics, flavonoids, and meliacins, potentially targeting multiple signaling pathways of cancer cells[3,4]. Extract of neem leaves have been reported to be non-toxic, non-mutagenic and found to possess immunomodulatory, anti-inflammatory and anticarcinogenic properties[5,6]. Neem leaf glycoprotein exhibited anti-tumor activity by activation of cytotoxic T lymphocytes and natural killer cells in patients with head and neck squamous cell carcinoma[7]. The neem limonoids (azadirachtin and nimbolide) reported to have an inhibitory effect on hamster cheek pouch carcinogenesis[8].

Nanotechnology has witnessed significant progress in the past few decades and its effect is widespread nowadays in every field. It is rapidly evolving and expanding discipline that has gained public and media interest worldwide. The use of nanotechnology in cancer biology has provided hope within the scientific community for developing novel cancer therapeutic strategies. Nanoparticles can be modified in numerous ways to prolong circulation, enhance drug localization, increase drug efficacy, and potentially decrease the chances of multi-drug resistance through the use of nanotechnology[1].

Cancer nanotechnology is a rapidly growing field and has made a remarkable contribution to treatment strategies by enabling the site-specific release of chemotherapeutic agents based on their physicochemical characteristics and biological attributes. Several therapeutic nanoparticle formulations showed high stability and carrier capacity which were found suitable for administration of both hydrophilic and hydrophobic drugs by various routes[9-11]. Calcium phosphate is a natural biomineral and therefore possesses an excellent biocompatibility due to its chemical similarity to human hard tissues such as bone and teeth. Calcium phosphate nanoparticles can be precipitated under controlled conditions and used as carrier in biological systems, e.g., to transfer nucleic acids or drugs[12].

Hence, the present study was designed to test the anticancer activity of neem (*A. indica*) leaf extract and its combination with calcium phosphate nanoparticles as an alternative medicine in chemoprevention of 7, 12-Dimethylbenzanthracene (DMBA) induced mammary carcinogenesis in rats.

2. Materials and Methods

2.1 Materials

A total of 54, 25-35 days old Sprague-Dawley virgin female rats, weighing 61 to 110 g were procured from the National Institute of Nutrition, Hyderabad. Alcoholic Neem (*Azadirachta indica*) leaf extract (NE) was procured from M/s. Natural Remedies, Private Limited, Bengaluru, India and stored at room temperature. Calcium chloride, sodium phosphate dibasic, sodium citrate tribasic dihydrate and DMBA were purchased from M/s. Sigma Aldrich Inc., St. Louis, USA and stored at room temperature. Olive oil was procured from local market and used as vehicle for administration of DMBA. Phosphate buffer saline (PBS, pH-7.4) was used as vehicle for administration of nanoparticles.

2.2 Methods

2.2.1 Synthesis of Neem Extract Loaded Calcium Phosphate Nanoparticles

Void calcium phosphate nanoparticles (CaNP) were synthesized as per standard protocol mentioned by earlier research workers[13]. Neem leaf Extract (NE) powder (1600mg) was dissolved in 80mL triple distilled water and stirred for 30 minutes on magnetic stirrer at 1000 rpm and initial OD was measured at wavelength $\lambda = 620$ AU. Dissolved NE (60mL, pH-5.33) was added to sodium

citrate (15.6mM, 30mL) in stirring mode. Calcium chloride (300Mm, 30mL) and dibasic sodium phosphate (300mM, 30mL) were slowly added to the above mixture drop by drop in stirring mode and final pH of mixture was adjusted to 7.4 and stirred for 4-5 hours (h) at 1200rpm. The resultant mixture was centrifuged at 9000 rpm for 15 min and the final OD of supernatant was measured at wavelength λ = 620 AU. The pellet was washed 2-3 times with PBS (pH-7.4) and dried in the hot air oven for 4h at 60°C. The dried pellet was grounded into fine powder and stored in airtight bottle. This powder was used for further characterization as neem extract loaded calcium phosphate nanoparticles.

2.2.2 Estimation of Coupling/Loading/Binding Efficiency or Capacity of Nanoparticles

The neem extract was prepared as per protocol given above. Initial OD of neem extract was measured at λ = 620 AU on spectrophotometer. Neem extract loaded calcium phosphate nanoparticles (NE-CaNP) were synthesized as per the protocol given above. After centrifugation, the final OD of supernatant measured. The estimation of coupling/loading efficiency of synthesized nanoparticles was estimated as per the procedure given below:

1) Amount of uncoupled extract (b) = {Total Amount of Neem Extract Dissolved (a) / Initial OD of Neem Extract} x OD of Supernatant after Centrifugation
2) Amount of coupled extract (c) = a – b
3) Coupling efficiency of CaNP (%) = (c/a) x100

2.2.3 Characterization of NE-CaNP

The techniques used to characterize the void calcium phosphate nanoparticles and neem extract loaded calcium phosphate nanoparticles included Transmission Electron Microscopy (TEM) to know the surface morphology and Dynamic Light Scattering (DLS) technique for particle size and Zeta potential analysis. The presence of characteristic functional groups for void CaNP and NE-CaNP was analyzed by Fourier Transform Infrared Spectroscopy (FTIR) in the range of 400-4000 cm^{-1}. The qualitative phase content of synthesized CaNP and NE-CaNP was analyzed by X-Ray Diffraction (XRD) technique for the presence of characteristic peaks for calcium phosphate.

2.2.4 Experimental Trial and Ethical Approval

The experimental trial was approved by Institutional Animal Ethical Committee (IAEC) of Tamil Nadu Veterinary and Animal Sciences University vide approval Lr. No. 3957/DFBS/B/2012 dated 18.01.2013. All the experimental procedures were performed under the ethical guidelines for animal care as per the norms laid by Committee for the Purpose of Control and Supervision of Experiments on Animals (CPCSEA). The details of experimental design are given below:

A total of 54 female Sprague-Dawley rats were randomized and divided into five groups based on their body weight (g). The 210 mg of DMBA was dissolved in 42 ml of olive oil (concentration of DMBA: 5mg/ml of olive oil). Starting at 42nd day of age, the animals of the groups III, IV and V were administered with DMBA dissolved in olive oil @ 5 mg/animal once in a week for a period of 4 weeks by oral gavages. From the day of first dosing of DMBA, NE and NE-CaNP dispersed in phosphate buffer saline (PBS, pH-7.4) were given 3 times in a week to groups IV and V, respectively at their respective doses (Table 1) by oral gavages till the end of 21 weeks study. The animals were monitored daily for general clinical signs and mortality. Rats from each group anaesthetised by using halothane inhalation anaesthesia and sacrificed by exsanguination method on 150th day after initial dose of DMBA administration.

Table 1. Experimental design

Groups	Treatments	Dose	No. of Animals
I	Control	----	06
II	NE-CaNP Control	Neem Leaf Extract Loaded Calcium Phosphate Nanoparticles @ 200 mg/kg BW/thrice a week/p.o	06
III	DMBA	5 mg/animal/week/p.o for 4 weeks	14
IV	DMBA + NE	Neem Extract @ 200 mg/kg BW/thrice a week/p.o	14
V	DMBA + NE-CaNP	Neem Extract Loaded on Calcium Phosphate Nanoparticles @ 200mg/kg BW/thrice a week/p.o	14

2.2.5 Tumor Incidence Parameters

One week after administration of last dose of DMBA, all animals were palpated daily to monitor mammary tumor appearance and growth. The time of appearance of the first tumor (Latency period in days) and the location of every tumor by specific mammary gland (Six ventrolateral pairs-R1-R6 and L1-L6) were recorded. The number of rats with tumors (Tumor incidence) and the number of tumors per rat (Tumor frequency) on a weekly basis were also calculated till the end of study. The two largest diameters (mm) of each tumor were measured weekly using a digital calliper (M/s Mitutoyo Corporation, Japan) at the end of 21 weeks observation period and the tumor volume (mm^3) was calculated using the formula given by earlier reserchers[14] as mentioned below:

Tumor volume (mm^3) = (a x b^2)/2 (Where, a = larger diameter and b = smaller diameter)

2.2.6 Histopathological Evaluation

Rats from each group anaesthetised by using halothane inhalation anaesthesia and sacrificed by exsanguination method on 150th day after initial dose of DMBA administration. A detailed postmortem was conducted on sacrificed rats. All the internal organs were examined for any evidence of metastasis. Gross pathology of the mammary tumor was observed and recorded. The excised mammary tumor samples were fixed in 10 per cent neutral-buffered formalin and embedded in paraffin wax. The sections with 4-5 µm thickness were cut and subjected to hematoxylin and eosin (H and E) staining for histopathological study as per the conventional procedure. Mammary tumors were classified histologically according to the criteria outlined in previous studies[15,16].

Scarff-Bloom-Richardson scheme was applied for grading of mammary tumors based on the assessment of morphological parameters described in rat mammary carcinomas like structural pattern, stromal response, mast cell infiltration, secretion and micro cribriform pattern. Scores and grades were assigned to each mammary tumor accordingly as per the protocol described in earlier research works[17].

2.2.7 Statistical Analysis

The data generated for different parameters of the experimental study were subjected to one-way Analysis of Variance (ANOVA) test using IBM SPSS software version 20 for windows.

3. Results

3.1 Characterization of CaNP and NE-CaNP

The CaNP and NE-CaNP were found to be smooth, spherical with a tendency to agglomerate and evenly distributed under transmission electron microscopy. Dynamic Light Scattering (DLS) analysis revealed that the void CaNP and NE-CaNP had a mean diameter of 55.50 ± 14.60 nm (Mode 53.50 nm) and 231.4 ± 89.2 nm (Mode: 205.0 nm), respectively. The zeta potential of void CaNP and NE-CaNP were -22.10mV and -31.3mV, respectively. This demonstrated that the nanoparticle dispersion prepared in this study was physically stable system. The mean encapsulation or coupling efficiency of CaNP was found to be 90-91 %.

The presence of characteristic functional groups for void CaNP and NE-CaNP were analyzed by Fourier Transform Infrared Spectroscopy (FTIR) in the range of 400-4000 cm^{-1}. The FTIR analysis of void CaNP revealed the presence of characteristic bands assigned to phosphate group (470, 550, 600, 960, 1040, 1100 cm^{-1}) and hydroxyl group (632, 3572 cm^{-1}). The FTIR analysis of NE-CaNP revealed presence of characteristic bands for different functional groups for both CaNP assigned to phosphate group (470, 550, 600, 960, 1040, 1100 cm^{-1}), hydroxyl group (632, 3572 cm^{-1}) and for neem extract assigned to -OH (3600), -NH_2 (3399), =CH (3297), C=N and C=C (1656) and C=O (1688) groups.

The qualitative phase content of synthesized CaNP and NE-CaNP was analyzed by XRD for the presence of characteristic peaks for calcium phosphate. The XRD diffractograms of the void CaNP powder showed characteristic peaks of CaNP (2θ = 25.76°, 28.16°, 31.86°, 40.04°) were found in the spectrum. The XRD analysis of NE-CaNP showed all characteristic peaks of void CaNP with no significant shifting of peak positions. A markedly increase broadening of the XRD peaks of NE-CaNP powder strongly indicated an important reduction in the crystalline structure of the particles.

3.2 Tumor Latency

The mean latency period for occurrence of mammary tumor in the DMBA, DMBA+NE and DMBA+NE-CaNP groups was 57.43 ± 2.06, 71.86 ± 2.36 and 84.92 ± 4.18 days respectively. A significant (P≤0.05) difference was observed among the mean latency periods of DMBA,

Table 2. Mean (± SE) of latency period of mammary tumor development in the DMBA, DMBA+NE and DMBA+NE-CaNP treated female Sprague-Dawley rats

S. No.	Groups	Number of Animals with Tumor	Tumor Latency (Days)
1.	Control	0	0.00 ± 0.000
2.	NE-CaNP control	0	0.00 ± 0.00
3.	DMBA	14	57.43^{a} ± 2.06
4.	DMBA+NE	014	71.86^{b} ± 2.36
5.	DMBA+NE-CaNP	13	84.92^{c} ± 4.18

Means with different superscripts within a same column differ significantly from each other (P ≤ 0.05). Abbreviations: **DMBA**: 7, 2-Dimethylbenzanthracene, **NE**: Neem Leaf Extract, **NE-CaNP**: Neem Leaf Extract Loaded Calcium Phosphate Nanoparticles.

DMBA+NE and DMBA+NE-CaNP treated rats. There was a significant (P<0.05) increase in the latency period in the DMBA+NE and DMBA+NE-CaNP treated groups as compared with DMBA group. The difference was also significant (P ≤ 0.05) in the DMBA+NE-CaNP group when compared to the DMBA+NE group rats (Table 2).

3.3 Tumor Incidence

No tumor was observed in the control animals (0/12). In the DMBA and DMBA+NE treated groups, all 14/14 (100%) rats showed development of mammary tumors while in the DMBA+NE-CaNP treated group, 13/14 (92.86%) rats revealed mammary tumors.

3.4 Tumor Frequency

The mean tumor frequency for the DMBA, DMBA+NE and DMBA+NE-CaNP treated groups were 6.86 ± 0.78, 4.93 ± 0.49 and 4.69 ± 0.57 respectively. A significant (P≤0.05) difference was observed among the mean tumor frequency of DMBA, DMBA+NE and DMBA+NE-CaNP treated rats. There was a significant (P<0.05) decrease in the tumour frequency in the DMBA+NE and DMBA+NE-CaNP groups as compared to the DMBA group (Table 3).

3.5 Tumor Size and Volume

Mean tumor size (length and width) in the DMBA, DMBA+NE and DMBA+NE-CaNP groups were 20.06 ± 1.22, 16.48 ± 1.28, 14.01±0.83 and 15.33 ± 0.90, 13.34 ± 1.11 and 10.61 ± 0.69 mm, respectively. A significant (P<0.05) difference was observed among the tumor size of DMBA, DMBA+NE and DMBA+NE-CaNP treated rats. There was a significant (P ≤ 0.05) decrease in the tumor length and width in the DMBA+NE and DMBA+NE-CaNP groups as compared to the DMBA group (Table 4).

Mean tumor volume in the DMBA, DMBA+NE and DMBA+NE-CaNP groups were 5103.75 ± 1089.16,

Table 3. Mean (± SE) of frequency of mammary tumor occurrence in the DMBA, DMBA+NE and DMBA+NE-CaNP treated female Sprague-Dawley rats

S. No.	Groups	Number of Tumor Bearing Animals	Total number of Tumors	Tumor Frequency
1.	Control	0	0	0.00 ± 0.00
2.	NE-CaNP Control	0	0	0.00 ± 0.00
3.	DMBA	14	96	6.86^{b} ± 0.78
4.	DMBA+NE	14	69	4.93^{a} ± 0.49
5.	DMBA+NE-CaNP	13	61	4.69^{a} ± 0.57

Means with different superscripts within a same column differ significantly from each other (P ≤ 0.05). Abbreviations: **DMBA**: 7, 9Leaf Extract Loaded Calcium Phosphate Nanoparticles.

Table 4. Mean (± SE) tumor size (mm) and volume (mm^3) of mammary tumors in the DMBA, DMBA+NE and DMBA+NE-CaNP treated female Sprague-Dawley rats

S. No.	Groups	Tumor Length (a) (mm)	Tumor Width (b) (mm)	Tumor Volume (mm^3)	Percent Reduction in Volume
1.	Control	0.00 ± 0.00	0.00 ± 0.00	0.00 ± 0.00	-
2.	NE-CaNP control	0.00 ± 0.00	0.00 ± 0.00	0.00 ± 0.00	-
3.	DMBA	20.06b ± 1.22	15.33b ± 0.90	5103.75b ± 1089.16	100
4.	DMBA+NE	16.48a ± 1.28	13.34b ± 1.11	4036.96ab ± 1105.50	21
5.	DMBA+NE-CaNP	14.01a ± 0.83	10.61a ± 0.69	1325.10a ± 275.50	74

Means with different superscripts within a same column differ significantly from each other (P ≤ 0.05). Abbreviations: **DMBA**: 7, 2-Dimethylbenzanthracene, **NE**: Neem Leaf Extract, **NE-CaNP**: Neem Leaf Extract Loaded Calcium Phosphate Nanoparticles.

Table 5. Mean (± SE) tumor weight (g) of mammary tumors in the DMBA, DMBA+NE and DMBA+NE-CaNP treated female Sprague-Dawley rats

S. No.	Groups	Number of Tumor Bearing Rats	Tumor Weight (g)
1.	Control	0	0.00 ± 0.00
2.	NE-CaNP control	0	0.00 ± 0.00
3.	DMBA	14	5.11b ± 0.94
4.	DMBA+NE	14	3.73ab ± 0.94
5.	DMBA+NE-CaNP	13	1.31a ± 0.25

Means with different superscripts within a same column differ significantly from each other (P ≤ 0.05). Abbreviations: **DMBA**: 7, 2-Dimethylbenzanthracene, **NE**: Neem Leaf Extract, **NE-CaNP**: Neem Leaf Extract Loaded Calcium Phosphate Nanoparticles.

4036.96 ± 1105.50 and 1325.10 ± 275.50 mm^3, respectively. A significant (P<0.05) difference was observed in the tumor volume among DMBA, DMBA+NE and DMBA+NE-CaNP treated rats. In the DMBA+NE-CaNP group, significant (P ≤ 0.05) decrease in the volume of tumor was recorded as compared to the DMBA group.

3.6 Tumor Weight

Mean tumor weight in the DMBA, DMBA+NE and DMBA+NE-CaNP groups were 5.11 ± 0.94, 3.73 ± 0.94 and 1.31 ± 0.25 g, respectively. A significant (P ≤ 0.05) difference was observed among the tumor weight of DMBA, DMBA+NE and DMBA+NE-CaNP treated rats. There was significant (P ≤ 0.05) decrease in the tumor weight in the DMBA+NE-CaNP group as compared to the DMBA group (Table 5).

3.7 Gross and Histopathological Evaluation

Grossly, mammary tumors in the DMBA, DMBA+NE and DMBA+NE-CaNP groups were greyish white in colour, single to multilobulated, circumscribed and located subcutaneously and generally non-adherent to the subcutis. The tumors in the DMBA group were larger in size (20.06 x 15.33 mm, 5.11 g) (Figures 1(a)-(b), Figure 3(a)) as compared to the DMBA+NE and DMBA+NE-CaNP groups and cut surfaces were uneven greyish white or creamy white or yellowish in colour, multilobulated and showed larger necrotic and haemorrhagic areas (Figure 3(b)) while the tumors in the DMBA+ NE (16.48 x 13.34 mm, 3.73 g) and DMBA+ NE-CaNP (14.01 x 10.61 mm, 1.31 g) groups were smaller in size (Figures 2(a)-(b), Figure 3(c)), less lobulated and cut surfaces were smooth whitish yellow in colour with even surfaces having less lobulations with minimal or absence of necrotic or haemorrhagic areas (Figure 3(d)). Metastatic lesions were observed in the spleen of a rat from DMBA group.

Out of 226 mammary tumors recorded, 96 were found in the DMBA, 69 in the DMBA+NE and 61 in the DMBA+NE-CaNP group rats. Out of 226 mammary tumors, 84 were benign and 142 were malignant tumors. The respective incidence of benign tumors was 26

(27.10%), 29 (42.03%) and 29 (47.54%) and malignant tumors were 70 (72.90%), 40 (57.97%) and 32 (52.46%) in the DMBA, DMBA+NE and DMBA+NE-CaNP group rats, respectively. The relative percent reduction in malignancy as compared to the DMBA group was 42.86% and 54.29% in the DMBA+NE and DMBA+NE-CaNP groups, respectively (Table 6).

Among 26 benign lesions recorded in DMBA group were comprised of 3 (11.54%), 6 (23.08%), 2 (7.69%) and 15 (57.69%) were hyperplasia, adenomas, fibromas and fibroadenomas, respectively. Among 70 malignant lesions, 67 (95.71%) were adenocarcinomas (cribriform, comedo, tubular, papillary and secretory variants) and 3 (4.29%) were adenocarcinomas arising from fibroadenomas (Table 7 and Figures 4(a)-(d)). The malignant lesions from DMBA group rats also showed presence of marked anisocytosis, anisokaryosis, frequent mitoses, nuclear indentation, adjacent muscle invasion, calcification and multinucleated tumor giant cells. The metastases within liver and spleen were evident in few cases.

Among 29 benign lesions recorded in DMBA+NE group were comprised of 4 (13.79%), 7 (24.14%), 2 (6.90%) and 16 (55.17%) were hyperplasia, adenomas, fibromas and fibroadenomas, respectively. Out of 40 malignant lesions, 38 (95.00%) were adenocarcinomas and 2 (5.00%) were adenocarcinomas arising from fibroadenomas.

Among 29 benign lesions recorded in DMBA+NE-CaNP group were comprised of 6 (20.69%), 6 (20.69%), 5 (17.24%) and 12 (41.38%) were hyperplasia, adenomas, fibromas and fibroadenomas, respectively. In the DMBA+NE-CaNP group, out of 32 malignant lesions, 30 (93.75%) were adenocarcinomas and 2 (6.25%) were adenocarcinomas arising from fibroadenomas (Table 7 and Figures 5 (a)-(d)).

3.8 Analysis of Histopathological Parameters

Analysis of histopathological parameters of DMBA induced mammary tumors in DMBA+NE and DMBA+NE-CaNP groups in rat mammary carcinomas are presented in Table 8. In structural pattern, carcinomas with a prevailing cribriform pattern (100% to 70% of the tumor), carcinomas displaying similar rates between both patterns (60 to 40% of tumor with cribriform pattern) and carcinomas showing a predominant papillary pattern (30 to 0% of the tumor with a cribriform pattern) were found 82.87%, 14.28% and 2.85% in the DMBA group, 70%, 20% and 10% in the DMBA+NE group and 56.25%, 12.50% and 31.25% in the DMBA+NE-CaNP treated group, respectively. The highest and lowest percentage of cribriform pattern were observed in the DMBA and DMBA+NE-CaNP group, respectively (Figures 6(a)-(b)). As compared with other groups, the percentage of papillary pattern was found to be more in the DMBA+NE and DMBA+NE-CaNP group.

Stromal response was absent, light (+), moderate (++) and pronounced (+++) in 12.86%, 64.29%, 18.57% and 4.28% in the DMBA group, 5%, 60%, 25% and 10% in the DMBA+NE group and 3.12%, 50%, 34.28% and 12.5% in the DMBA+NE-CaNP treated group, respectively. The light and moderate stromal response observed in all groups but pronounced stromal response was observed in the DMBA+NE-CaNP group as compared to other groups (Figures 6 (c)-(d)).

Table 6. Nature of mammary tumors in the DMBA, DMBA+NE and DMBA+NE-CaNP treated female Sprague-Dawley rats and percentage reduction in malignancy

Groups	DMBA		DMBA+NE		DMBA+NE-CaNP	
Total number of Tumors	96		69		61	
Nature of Tumors (number)	Malignant	Benign	Malignant	Benign	Malignant	Benign
	70	26	40	29	32	29
Percentage	72.90	27.10	57.97	42.03	52.46	47.54
Relative Percentage	100	100	57.14	111.54	45.71	111.54
Per cent Reduction in Malignancy	100	---	42.86	---	54.29	---

Abbreviations: **DMBA**: 7, 12-Dimethylbenzanthracene, **NE**: Neem Leaf Extract, **NE-CaNP**: Neem Leaf Extract Loaded Calcium Phosphate Nanoparticles.

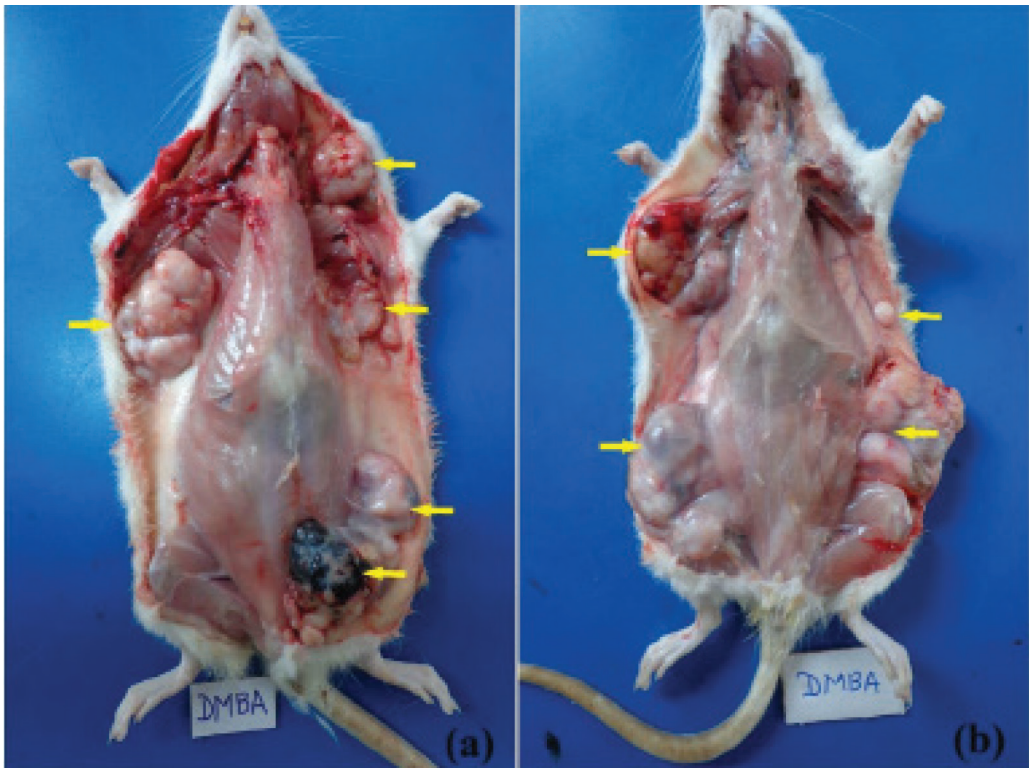
Table 7. Histopathological evaluation of DMBA induced mammary lesions in the DMBA, DMBA+NE and DMBA+NE-CaNP treated female Sprague-Dawley rats

Lesion	DMBA	DMBA+NE	DMBA+NE-CaNP
Total Number of Lesions	96	69	61
A) Benign Lesions	26	29	29
Hyperplasia	3 (11.54%)	4 (13.79%)	6 (20.69%)
Adenoma	6 (23.08%)	7 (24.14%)	6 (20.69%)
Fibroma	2 (7.69%)	2 (6.90%)	5 (17.24%)
Fibroadenoma	15 (57.69%)	16 (55.17%)	12 (41.38%)
B) Malignant Lesions	70	40	32
Adenocarcinoma	67 (95.71%)	38 (95.00%)	30 (93.75%)
Adenocarcinoma arising from fibroadenoma	3 (4.29%)	2 (5.00%)	2 (6.25%)

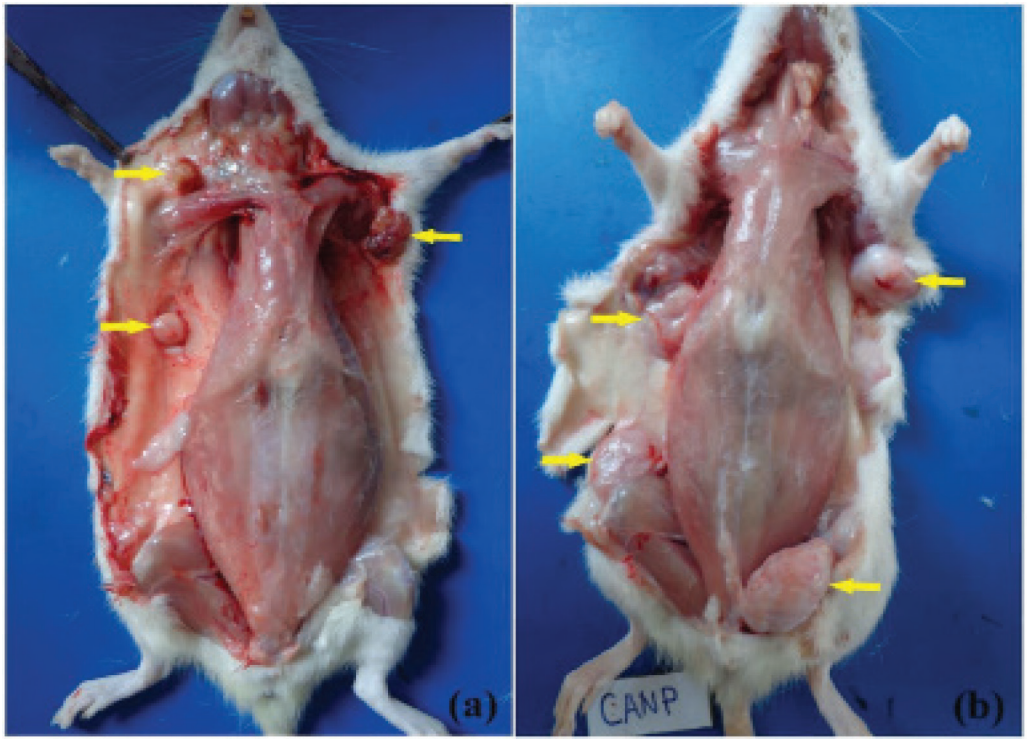
Abbreviations: **DMBA**: 7, 12-Dimethylbenzanthracene, **NE**: Neem Leaf Extract, **NE-CaNP**: Neem Leaf Extract Loaded Calcium Phosphate Nanoparticles.

Mast cell infiltration was absent, light (+), moderate (++) and pronounced (+++) in 0%, 52.86%, 40% and 7.14% in the DMBA group, 0%, 42.5%, 50% and 7.5% in the DMBA+NE group and 0%, 34.38%, 50% and 15.62% in the DMBA+NE-CaNP treated group, respectively. Absence of mast cell infiltration was not found in any of the treatment groups while light to moderate infiltrations were observed in all groups. Pronounced mast cell infiltration was seen in the DMBA+NE-CaNP group (Figures 7 (a)-(b)).

Secretion in carcinomas was absent, focal and widespread in 60%, 30% and 10% in the DMBA group, 50%, 35% and 15% in the DMBA+NE group and 25%, 40% and 35% in the DMBA+NE-CaNP treated group, respectively (Figures 7 (c)-(d)).



Figures 1. **(a)** and **(b)** DMBA Group: Large greyish-white multi-lobulated mammary growths (arrows).



Figures 2. **(a)** and **(b)** DMBA+NE-CaNP Group: Small sized less lobulated mammary growths (arrows).

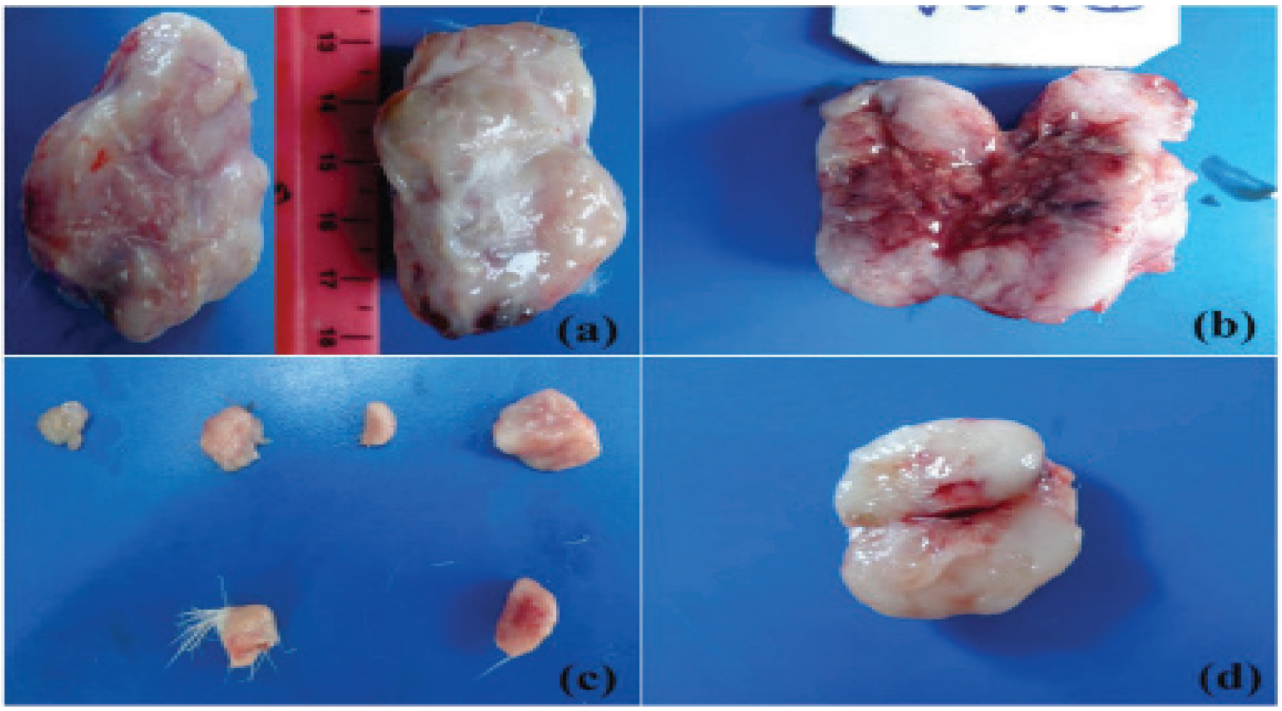


Figure 3. **(a)** DMBA Group: Excised large greyish-white multi-lobulated mammary growths. **(b)** DMBA Group: Cut surface showing multi-nodular necro-haemorrhagic changes in mammary growths. **(c)** DMBA+NE-CaNP Group: Small sized greyish-white nodules to minimally lobulated mammary growths. **(d)** DMBA+NE-CaNP Group: Greyish white less nodular even surfaced mammary growth.

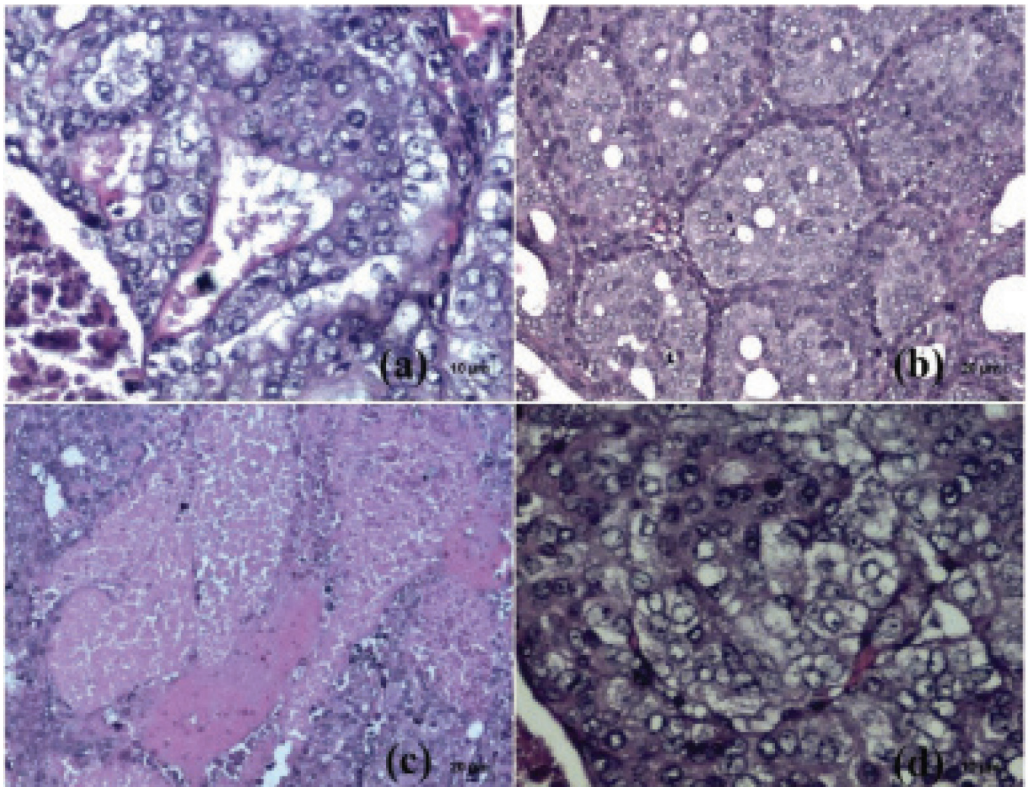


Figure 4. **(a)** DMBA Group: Tubular adenocarcinoma: Presence of uniform one to several cell layers thick neoplastic epithelial cells lining the tubules with small and empty tubular lumina (H and E stain, Bar = 10µm). **(b)** DMBA Group: Cribriform adenocarcinoma: Sieve-like pattern due to numerous secondary lumina which are small, round spaces, often filled with proteinaceous secretion and dispersed throughout the solid tumor mass. (H and E stain, Bar = 20µm). **(c)** DMBA Group: Comedo-carcinoma: Distended ductules filled with sheets of neoplastic cells which have become centrally necrotic. The central cavity contains cellular debris. (H and E stain, Bar = 20µm). **(d)** DMBA Group: Tubular adenocarcinoma: Note marked anisocytosis and anisokaryosis (H and E stain, Bar = 10µm).

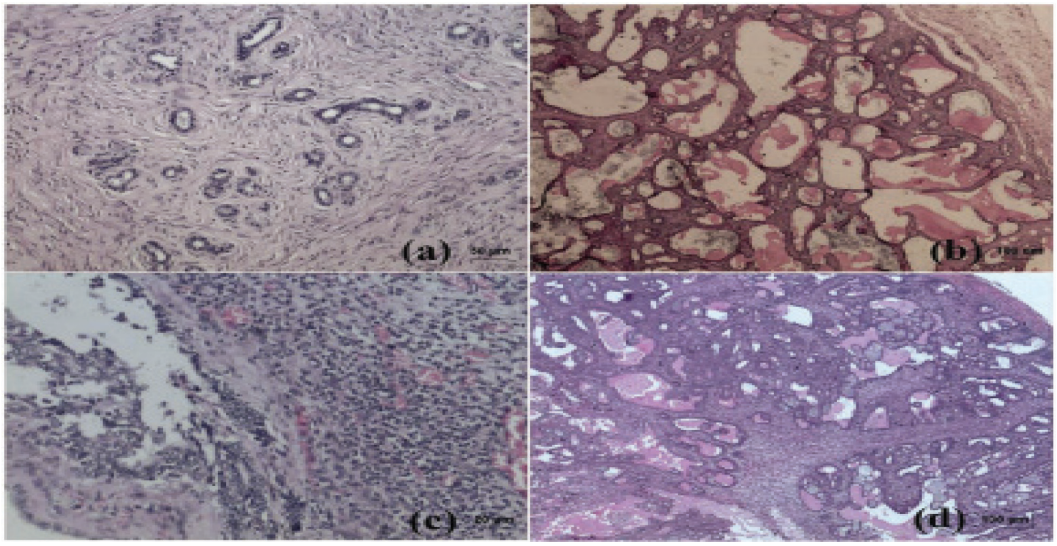


Figure 5. **(a)** DMBA+NE-CaNP Group: Fibroadenoma (H and E stain, Bar = 50µm). **(b)** DMBA+NE-CaNP Group: Secretory cystadenoma (H and E stain, Bar = 100µm). **(c)** DMBA+NE-CaNP: Adenoma: Note marked lymphoplasmacytic infiltration (H and E stain, Bar = 20µm). **(d)** DMBA+NE-CaNP Group: Secretory tubular adenocarcinoma (H and E stain, Bar = 100µm).

Table 8. Analysis of histopathological parameters in the DMBA, DMBA+NE and DMBA+NE-CaNP treated female Sprague Dawley rat as previously described in rat mammary carcinomas

Histologic Parameters	DMBA	DMBA+NE	DMBA+NE-CaNP
Structural Pattern (%)			
Carcinomas with a prevailing cribriform pattern (100% to 70% of the tumor)	82.87	70	56.25
Carcinomas displaying similar rates between both patterns (60% to 40% of the tumor with a cribriform pattern)	14.28	20	12.50
Carcinomas showing a predominant papillary pattern (30% to 0% of the tumor with a cribriform pattern)	2.85	10	31.25
Stromal Response (%)			
Absent	12.86	5	3.12
+	64.29	60	50
++	18.57	25	34.38
+++	4.28	10	12.5
Mast Cell Infiltration (%)			
Absent	0	0	0
+	52.86	42.5	34.38
++	40	50	50
+++	7.14	7.5	15.62
Secretion in Carcinomas (%)			
Absent	60	50	25
Focal	30	35	40
Widespread	10	15	35
Microcribriform Pattern (%)			
Absent	80	55	15
Present	20	45	85

Abbreviations: **DMBA**: 7, 12-Dimethylbenzanthracene, **NE**: Neem Leaf Extract, **NE-CaNP**: Neem Leaf Extract Loaded Calcium Phosphate Nanoparticles.

Microcribriform pattern was absent and present in 80% and 20% in the DMBA group, 55% and 45% in the DMBA+NE group and 15% and 85% in the DMBA+NE-CaNP treated group, respectively.

Carcinomas with a prevailing cribriform pattern was mostly observed in the DMBA and DMBA+NE groups while the papillary pattern was predominantly observed in the DMBA+NE-CaNP group. Most of the carcinomas exhibited no stromal response in the DMBA group. The light to moderate stromal response was observed in all groups but pronounced stromal response was found in the DMBA+NE-CaNP group. Light mast cell infiltration was encountered primarily in the DMBA group. Light to moderate mast cell infiltration was seen in the all groups while pronounced mast cell infiltration was mostly found in the DMBA+NE-CaNP group. Majority of carcinomas in the DMBA group did not show any secretory activity. Focal secretion was observed in moderate level in carcinomas of all groups while carcinomas with widespread secretions were developed in the DMBA+NE-CaNP treated group. Micro cribriform pattern was mostly absent in the DMBA group while it was predominant in the carcinomas from DMBA+NE-CaNP group and was either present or absent in equal number in carcinomas of the DMBA+NE group.

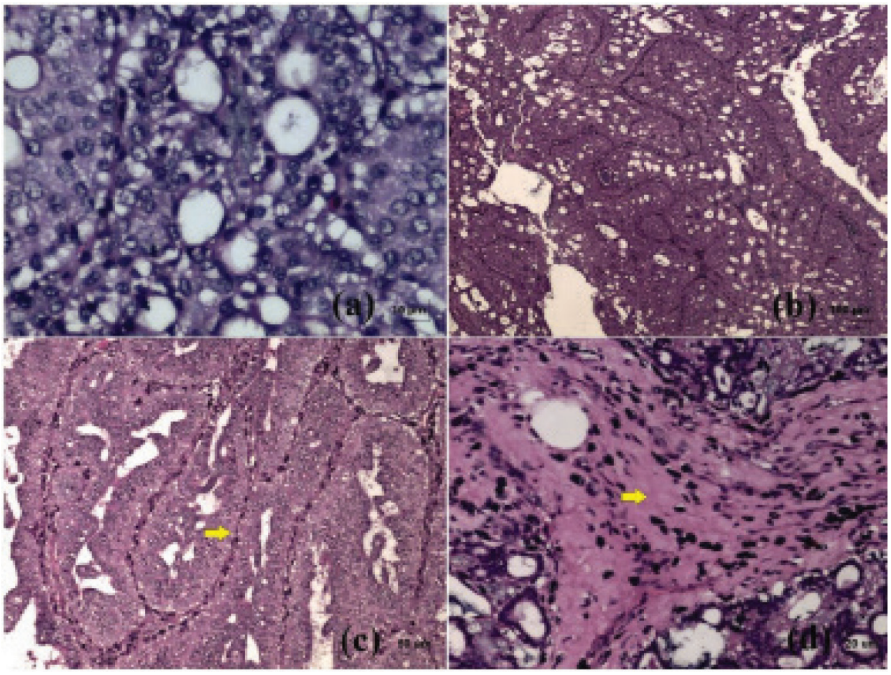


Figure 6. **(a)** DMBA Group: Cribriform adenocarcinoma: Note predominant sieve-like or cribriform structural pattern due to numerous secondary lumina which are small, round spaces, often filled with proteinaceous secretion and dispersed throughout the solid tumor mass (H and E stain, Bar = 10µm). **(b)** DMBA+NE-CaNP: Note Lower cribriform structural pattern (H and E stain, Bar = 100µm). **(c)** DMBA Group: Note Light (+) stromal response (arrow). (H and E stain, Bar = 50µm). **(d)** DMBA+NE-CaNP Group: Pronounced (+++) stromal response (arrow). (H and E stain, Bar = 20µm).

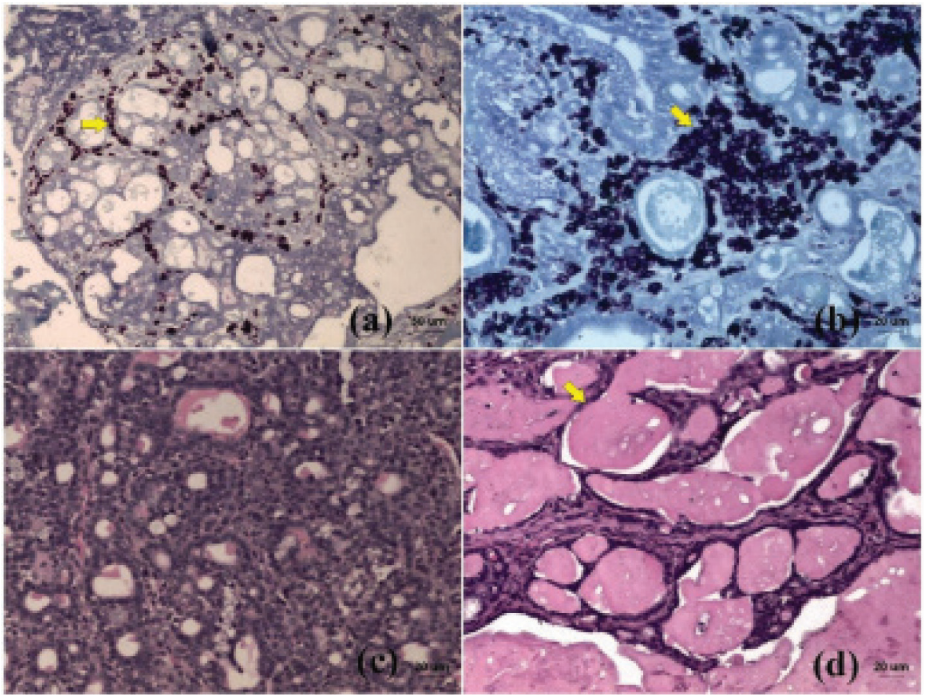


Figure 7. **(a)** DMBA Group: Note Light (+) mast cell infiltration (arrow). (Toluidine Blue stain, Bar = 50µm). **(b)** DMBA+NE-CaNP Group: Note Pronounced (+++) mast cell infiltration (arrow). (Toluidine Blue Stain, Bar = 20µm). **(c)** DMBA Group: Less micro cribriform pattern with focal secretion (H and E stain, Bar = 20µm). **(d)** DMBA+NE-CaNP Group: Widespread secretion (arrow). (H and E stain, Bar = 20µm).

4. Discussion

The CaNP and NE-CaNP were found to be smooth, spherical with a tendency to agglomerate and evenly distributed under transmission electron microscopy. These morphological findings observed in the present study are in agreement with findings reported by earlier workers[18-20]. Dynamic Light Scattering (DLS) analysis revealed that the void CaNP and NE-CaNP had a mean diameter of 55.50 ± 14.60 nm (Mode 53.50 nm) and 231.4 ± 89.2 nm (Mode: 205.0 nm) respectively. The zeta potential of void CaNP and NE-CaNP were -22.10 mV and -31.3 mV respectively. This demonstrated that the nanoparticle dispersion prepared in this study was physically stable system. The methazolamide-loaded CaP nanoparticles had a zeta potential of about -30.4 ± 2.2 mV while their mean particle diameter was 256.4 ± 31.1 nm[21]. The DLS analysis revealed the antigen (SP) protein adsorbed CaP nanoparticles and CaP nanoparticles had an average diameter of 224.98 ± 14.62 nm and 200.44 ± 18.62 nm and zeta potential of the CaP nanoparticles and SP adsorbed CaP nanoparticles was -21.65 ± 2.6 and -34.81 ± 3 mV, respectively[19].

The mean encapsulation or coupling efficiency of CaNP was found to be 90-91 %. This was in agreement with the results of earlier workers who reported an adsorption efficiency of 95.9 ± 3.5% of antigen protein (SP) on CaP nanoparticles[19]. The findings recorded regarding FTIR analysis of CaNP nanoparticles and neem extract were also in agreement with earlier reports by various researchers[18,22-24]. XRD analyses showed characteristic peaks of CaNP (2θ = 25.76°, 28.16°, 31.86°, 40.04°) and NE-CaNP showed all characteristic peaks of void CaNP with no significant shifting of peak positions. A marked broadening increase of the XRD peaks of NE-CaNP powder strongly indicated an important reduction in the crystalline structure of the particles. The findings of XRD analysis for CaNP are in consonance with the findings observed in various previous studies reports[21-23].

No tumor was encountered in the control animals (0/12). In the DMBA and DMBA+NE treated groups, all 14/14 (100%) rats showed development of mammary tumors while in the DMBA+NE-CaNP treated group, 13/14 (92.86%) rats revealed mammary tumors. The earlier studies also reported induction of mammary tumors in 100% population of rats with a single oral dose of DMBA @ 20 mg and 80-100 mg/kg body weight, as well as significant reduction in mammary tumor incidence in neem flowers treated group as compared to the DMBA group[25-28].

First mammary tumor appeared on 48th day after first DMBA dosing in three animals in the DMBA group, in eight animals on 66th day in the DMBA+NE group and in eight rats 78th day in the DMBA+NE-CaNP treatment group. The mean latency periods for occurrence of mammary tumor in the DMBA, DMBA+NE and DMBA+NE-CaNP groups were 57.43 ± 2.06, 71.86 ± 2.36 and 84.92 ± 4.18 days, respectively. There was a significant increase in the latency period in the DMBA+NE and DMBA+NE-CaNP treated groups as compared with DMBA group. The difference was also significant in the DMBA+NE-CaNP group when compared to the DMBA+NE group rats. Earlier study showed that the latent period until the appearance of the first palpable tumor of mammary gland was slightly longer, although not significantly, in animals fed neem flowers (62.7 ± 18.5 days) compared to that in the DMBA control group (53.3 ± 8.8 days). However, the incidence of mammary gland tumors in neem flowers group slower than that in the DMBA control group. Lower multiplicity or frequency (the number of tumors per rat) as well as smaller size of mammary gland tumors recorded in neem flower group as compared to DMBA control animals and the difference lowered significantly at 14-17 weeks after the administration of DMBA[28].

The anti-carcinogenic potential of neem compounds may be attributable to one or more phytochemicals viz. azadirachtin, nimbolide, quercetin etc. through mechanisms such as antiproliferative, apoptotic and upregulation of antioxidant defences. Neem leaf fractions function as dual-acting agents by suppressing phase I enzymes and inhibiting metabolic activation of carcinogens, whilst simultaneously enhancing phase II enzyme activities thereby promoting detoxification and excretion[27,28]. Small size of nanoparticles endows them with properties such as less resistance of cancer stem cells to drug uptake, high surface area to volume ratio, accumulation at tumor sites, block drug efflux, targeted drug delivery and maximum bioavailability[1,9-12]. These properties of nanoparticles make them superior over conventional large sized drug molecules. In present study, the better anticarcinogenic effect observed in DMBA+NE-CaNP as compared to DMBA+NE group rats may be correlated with the combined potential of neem leaf extract and calcium phosphate nanoparticles due to above mentioned properties.

However, in present study, the neem leaf treatment significantly increased the latency period as compared to only DMBA treatment. The DMBA+NE-CaNP treatment delayed the first tumor occurrence significantly as compared to DMBA+NE group. Hence, nano formulation of neem extract has the advantage over alone neem extract treatment.

In the DMBA group, 96 mammary tumors (including 3 hyperplasia) were found in 14 affected rats. The DMBA+NE group rats showed 69 mammary tumors in the 14 tumor bearing animals. The DMBA+NE-CaNP treated group showed 61 mammary tumors in the 13 tumor bearing animals. The mean tumor frequency in the DMBA, DMBA+NE and DMBA+NE-CaNP treated groups were 6.86 ± 0.78, 4.93 ± 0.49 and 4.69 ± 0.57, respectively. There was a significant decrease in the tumor frequency in DMBA+NE and DMBA+NE-CaNP groups as compared to DMBA group. The results of DMBA induced mammary tumors concurred with earlier findings[29] who reported that the administration of 10 mg DMBA/rat, three times, at three days interval in 50-60 days-old virgin female Sprague-Dawley rats for 25 weeks produced mammary tumors with tumor frequency of 7.1. The lower multiplicity or frequency (the number of tumors per rat) of mammary gland tumors in neem flower group and the difference was significant at 14-17 weeks after the administration of DMBA[28].

Mean tumor size (length and width) in the DMBA, DMBA+NE and DMBA+NE-CaNP groups were 20.06 ± 1.22, 16.48 ± 1.28, 14.01 ± 0.83 and 15.33 ± 0.90, 13.34 ± 1.11 and 10.61 ± 0.69 mm, respectively. There was a significant decrease in the tumor length and width in DMBA+NE and DMBA+ NE-CaNP groups as compared to DMBA group. Mean tumor volume in the DMBA, DMBA+NE and DMBA+NE-CaNP groups were 5103.75 ± 1089.16, 4036.96 ± 1105.50 and 1325.10 ± 275.50 mm^3, respectively. In DMBA+NE-CaNP group, significant decrease in the tumor volume was recorded as compared to the DMBA group. Earlier researchers[29] also reported that the average tumor volume was 4360 ± 1990 mm^3 following administration of DMBA (10 mg/rat, three times) at three days interval in 50 to 60 days-old virgin female Sprague-Dawley rats for 25 weeks. However, lesser tumor volume of 2183.38 ± 634.15 mm^3 also reported in few studies[30], which might be due to lesser duration of (113 days) study. The findings regarding neem extract treatment observed in present study agreed with previous works[28] reporting smaller size of tumors in neem flowers fed group than the DMBA control animals. The present study revealed that NE-CaNP could reduce the mammary tumor volume to the extent of 74 percent compared to the DMBA group and 67 per cent compared to the NE. This showed the efficiency of NE-CaNP in reducing the tumor volume compared to NE alone treatment.

The gross appearance of DMBA induced mammary carcinomas were soft, fleshy, well vascularised with areas of necrosis and haemorrhage. Fibroadenomas were white with a rubbery and firm consistency and on sectioning shelled out from the capsule. The fibroadenomas were appeared non-encapsulated, round to oval masses and well circumscribed from the adjacent mammary parenchyma. These gross pathological observations of these earlier studies were also in agreement with findings of present study[16,17].

The earlier studies reported 68 per cent of mammary carcinoma and 32 per cent benign mammary tumors following administration of 20 mg of DMBA in Sprague-Dawley rats[25] while another study stated that 89 per cent of DMBA induced mammary tumors were adenocarcinomas and 11 per cent were fibroadenomas[31]. All the mammary carcinomas observed in the present study were adenocarcinomas, which is in agreement with findings of earlier researchers who reported that most of the DMBA induced tumors were malignant and epithelial in nature[17]. In present study, the tumors recorded were found to be originated from alveolar and or ductal epithelium. The various distinct patterns of adenocarcinomas observed in the present study included tubular pattern, papillary pattern, cribriform pattern, comedo pattern and adenocarcinoma arising from fibroadenoma. These histopathological findings were also in consonance with the observations of earlier researchers[15,16]. The present study revealed that NE treatment could decrease malignancy by 43 per cent whereas NE-CaNP treatment could decrease malignancy by 54% when compared to the DMBA control.

Mast cells accumulate in the stroma surrounding certain tumors especially mammary adenocarcinoma in reaction to tumor growth and in an effort to destroy the tumor by secreting molecules such as IL-4 (that induces apoptosis), TNF-α (that kills tumor cells) or tryptase that stimulates protease-activated receptor-induced inflammation[32]. The higher mast cell count can be correlated with good prognosis of breast cancers and in rural setup where immune staining is not available, the mast cell count by to toluidine blue stain can be used as a screening procedure to determine the prognosis of breast cancers and their

sensitivity to hormonal therapy[33]. In present study, the light to moderate mast cell infiltration was seen in the all groups while pronounced mast cell infiltration was mostly found in the DMBA+NE-CaNP group indicating more tumor growth inhibition and good prognosis.

5. Conclusions

In conclusion, the neem leaf extract loaded calcium phosphate nanoparticles were found to have better anti-carcinogenic potential as it significantly reduced the incidence, frequency, weight, volume and malignancy of DMBA induced mammary tumors and increased the tumor latency period in Sprague-Dawley rats when compared to treatment with neem extract alone. Findings of the present study suggested that the neem leaf extract loaded calcium phosphate nanoparticles has immense potential to cure and prevent the mammary carcinogenesis. Preparation and development of neem leaf extract loaded calcium phosphate nanoparticles may future potential candidate for anticancer therapeutics.

6. Acknowledgements

The authors thank Tamil Nadu Veterinary and Animal Sciences University, Chennai for providing necessary facilities and assistance to conduct this study.

7. References

1. Jabir NR, Tabrez S, Ashraf GM, Shakil S, Damanhouri GA, Kamal MA. Nanotechnology-based approaches in anticancer research. Int J Nanomedicine. 2012; 7:4391-08. https://doi.org/10.2147/IJN.S33838
2. Desai AG, Qazi GN, Ganju RK, El-Tamer M, Singh J, Saxena AK. Medicinal plants and cancer chemoprevention. Curr Drug Metab. 2008; 9:581-91. https://doi.org/10.2174/138920008785821657
3. Bose A, Chakraborty K, Sarkar K, Goswami S, Chakraborty T, Pal S. Neem leaf glycoprotein induces perforin-mediated tumor cell killing by T and NK cells through differential regulation of IFN-gamma signaling. J Immunother. 2009; 32:42-53. https://doi.org/10.1097/CJI.0b013e31818e997d
4. Sarkar K, Bose A, Haque E, Chakraborty K, Chakraborty T, Goswami S. Induction of type 1 cytokines during neem leaf glycoprotein assisted carcinoembryonic antigen vaccination is associated with nitric oxide production. Int Immunopharmacol. 2009; 9:753-60. https://doi.org/10.1016/j.intimp.2009.02.016
5. Haque E, Mandal I, Pal S, Baral R. Prophylactic dose of neem (*Azadirachta indica*) leaf preparation restricting murine tumor growth is non-toxic, hematostimulatory and immunostimulatory. Immunopharmacol Immunotoxicol. 2006; 28:33-50. https://doi.org/10.1080/08923970600623632
6. Chakraborty K, Bose A, Pal S, Sarkar K, Goswami S, Ghosh D. Neem leaf glycoprotein restores the impaired chemotactic activity of peripheral blood mononuclear cells from head and neck squamous cell carcinoma patients by maintaining CXCR3/ CXCL10 balance. Int Immunopharmacol. 2008; 8:330-40. https://doi.org/10.1016/j.intimp.2007.10.015
7. Bose A, Chakraborty K, Sarkar K, Goswami S, Haque E, Chakraborty T. Neem leaf glycoprotein directs T-bet-associated type 1 immune commitment. Hum Immunol. 2009; 70:6-15. https://doi.org/10.1016/j.humimm.2008.09.004
8. Priyadarsini RV, Manikandan P, Kumar GH, Nagini S. The neem limonoids azadirachtin and nimbolide inhibit hamster cheek pouch carcinogenesis by modulating xenobiotic-metabolizing enzymes, DNA damage, antioxidants, invasion and angiogenesis. Free Radic Res. 2009; 43:492-04. https://doi.org/10.1080/10715760902870637
9. Gelperina S, Kisich K, Iseman MD, Heifets L. The potential advantages of nanoparticle drug delivery systems in chemotherapy of tuberculosis. Am J Respir Crit Care Med. 2005; 172:1487-90. https://doi.org/10.1164/rccm.200504-613PP
10. Cho K, Wang X, Nie S, Chen ZG, Shin DM. Therapeutic nanoparticles for drug delivery in cancer. Clin Cancer Res. 2008; 14:1310-16. https://doi.org/10.1158/1078-0432.CCR-07-1441
11. Ranganathan R, Madanmohan S, Kesavan A. Nanomedicine: Towards development of patient-friendly drug-delivery systems for oncological applications. Int J Nanomedicine. 2012; 7:1043-60. https://doi.org/10.2147/IJN.S25182
12. Epple M, Kovtun A. Functionalized calcium phosphate nanoparticles for biomedical application. Key Eng Mater. 2010; 441:299-05. https://doi.org/10.4028/www.scientific.net/KEM.441.299
13. He Q, Mitchell AR, Johnson SL, Wagner-Bartak C, Morcol T, Bell JD. Calcium Phosphate Nanoparticle Adjuvant. Clin Diagn Lab Immunol. 2000; 7:899-03. https://doi.org/10.1128/CDLI.7.6.899-903.2000
14. Carlsson G, Gullberg B, Hafstrom L. Estimation of liver tumor volume using different formulas - An experimental study in rats. J Cancer Res Clin. 1983; 105:20-23. https://doi.org/10.1007/BF00391826
15. Mann PC, Boorman GA, Lollini LO, McMartin DN, Goodman DG. Proliferative lesions of the mammary gland in rats, IS-2. In: Guides for Toxicologic Pathology. STP/ARP/AFIP Publishers, Washington DC, USA. 1996; 1-7.
16. Russo J, Russo IH. Atlas and histologic classification of tumors of the rat mammary gland. J Mammary

Gland Biol Neoplasia. 2000; 5:187-200. https://doi.org/10.1023/A:1026443305758
17. Costa I, Solanas M, Escrich E. Histopathologic characterization of mammary neoplastic lesions induced with 7, 12-dimethylbenz (a) anthracene in the rat. Arch Pathol Lab Med. 2002; 126:915-27. https://doi.org/10.5858/2002-126-0915-HCOMNL
18. Wang P, Li C, Gong H, Jiang X, Wang H, Li K. Effects of synthesis conditions on the morphology of CaP nanoparticles produced by wet chemical process. Powder Technol. 2010; 203:315-21. https://doi.org/10.1016/j.powtec.2010.05.023
19. Behera T, Swain P. Antigen adsorbed calcium phosphate nanoparticles stimulate both innate and adaptive immune response in fish (*Labeo rohita*). Cell Immunol. 2011; 271:350-59. https://doi.org/10.1016/j.cellimm.2011.07.015
20. Koppad S, Dhinakar Raj G, Gopinath VP, John Kirubaharan J, Thangavelu A, Thiagarajan V. Calcium phosphate coupled Newcastle disease vaccine elicits humoral and cell mediated immune responses in chickens. Res Vet Sci. 2011; 91:384-90. https://doi.org/10.1016/j.rvsc.2010.09.008
21. Chen R, Qian Y, Li R, Zhang Q, Liu D, Wang M, Xu Q. Methazolamide calcium phosphate nanoparticles in an ocular delivery system. Yakugaku Zasshi. 2010; 130:419-24. https://doi.org/10.1248/yakushi.130.419
22. Nimal TR. Development of extracellular matrix-nano hydroxyapatite composite scaffold for based bone tissue engineering. MTech thesis submitted to National Institute of Technology, Rourkela, India; 2013.
23. Mercado DF, Giuliana M, Malandrino M, Rubert AA, Montoneri E, Celi L, Prevot AB, Gonzalez MC. Paramagnetic iron-doped hydroxyapatite nanoparticles with improved metal sorption properties-A bio-organic substrates-mediated synthesis. ACS Appl Mater Interfaces. 2014; 6:3937-46. https://doi.org/10.1021/am405217j
24. Bhattacharyya KG, Sharma A. Adsorption of Pb (II) from aqueous solution by *Azadirachta indica* (neem) leaf powder. J Hazard Mater. 2004; 113:97-109. https://doi.org/10.1016/j.jhazmat.2004.05.034
25. Giganti DM, Niehans GA, Reichert MA, Bliss RL. Post-initiation treatment of rats with indole-3-carbinol or b-naphthoflavone does not suppress 7, 12-dimethylbenz[a] anthracene induced mammary gland carcinogenesis. Cancer Lett. 2000; 160:209-18. https://doi.org/10.1016/S0304-3835(00)00594-2
26. Russo IH, Russo J. Mammary gland neoplasia in long-term rodent studies. Environ Health Perspect. 1996; 104:938-67. https://doi.org/10.1289/ehp.96104938
27. Vinothini G, Manikandan P, Anandan R, Nagini S. Chemoprevention of rat mammary carcinogenesis by *Azadirachta indica* leaf fractions: Modulation of hormone status, xenobiotic-metabolizing enzymes, oxidative stress, cell proliferation and apoptosis. Food Chem Toxicol. 2009; 47:1852-63. https://doi.org/10.1016/j.fct.2009.04.045
28. Tepsuwan A, Kupradinun P, Kusamran WR. Chemopreventive potential of neem flowers on carcinogen-induced rat mammary and liver carcinogenesis. Asian Pacific J Cancer Prev. 2002; 3:231-38.
29. Ahlersova E, Ahlers I, Kubatka P, Bojkova B, Mocikova K, Gajdosova S, Onderkova HM. Melatonin and retinyl acetate as chemo preventives in DMBA-induced mammary carcinogenesis in female Sprague-Dawley rats. Folia Biol. 2000; 46:69-72.
30. Jalantha P. Pathological evaluation of anti-tumor effect of curcumin against experimentally induced mammary tumor in rats [MSc Thesis]. Chennai, India: Tamil Nadu Veterinary and Animal Sciences University; 2012.
31. Sachdev GP, Wen G, Martin B, Kishore GS, Fox OF. γ-glutamyl-transpeptidase in chemically induced rat mammary gland carcinogenesis in specific dietary states. Proc Okla Acad Sci. 1980; 60:1-4.
32. Conti P, Castellani ML, Durasamy K, Vincenzo S, Jacopo V, Stefano T, Filiberto M, Alessandro P, Lutiis MAD, Tagen M, Theoharides TC. Role of mast cells in tumor growth. Ann Clin Lab Sci. 2007; 37:315-22.
33. Jana S, Ghosh S, De A, Pal S, Sengupta S, Ghosh T. Quantitative analysis and comparison of mast cells in breast carcinomas and axillary lymph nodes. Clin Cancer Invest J. 2017; 6:214-18. https://doi.org/10.4103/ccij.ccij_52_17